THE JOURNAL OF BIOLOGICAL CHEMISTRY
Vol. 280, No. 23, Issue of June 10, pp. 22091–22101, 2005
Printed in U.S.A.

In Situ Photoactivation of a Caged Phosphotyrosine Peptide Derived from Focal Adhesion Kinase Temporarily Halts Lamellar Extension of Single Migrating Tumor Cells*

Received for publication, March 11, 2005
Published, JBC Papers in Press, April 6, 2005, DOI 10.1074/jbc.M502726200

David Humphrey‡§¶‖, Zenon Rajfur‡¶, M. Eugenio Vazquez¶‡‡, Danielle Scheswohl‡, Michael D. Schaller‡§, Ken Jacobson‡§ §§, and Barbara Imperiali**¶¶**

*From the ‡Department of Cell and Developmental Biology, §Lineberger Comprehensive Cancer Center, University of North Carolina at Chapel Hill, Chapel Hill, North Carolina 27599 and the Departments of **Chemistry and ¶¶Biology, Massachusetts Institute of Technology, Cambridge, Massachusetts 02139*

Focal adhesion kinase (FAK), a non-receptor tyrosine kinase, mediates integrin-based cell signaling by transferring signals regulating cell migration, adhesion, and survival from the extracellular matrix to the cytoplasm. Following autophosphorylation at tyrosine 397, FAK binds the Src homology 2 domains of Src and phosphoinositide 3-kinase, among several other possible binding partners. To further investigate the role of phosphorylated FAK in cell migration *in situ*, peptides comprising residues 391–406 of human FAK with caged phosphotyrosine 397 were synthesized. Although the caged phosphopeptides were stable to phosphatase activity, the free phosphopeptides showed a half-life of ~10–15 min in cell lysates. Migrating NBT-II cells (a rat bladder tumor cell line) were microinjected with the caged FAK peptide and locally photoactivated using a focused laser beam. The photoactivation of caged FAK peptide in 8-μm diameter spots over the cell body led to the temporary arrest of the leading edge migration within ~1 min of irradiation. In contrast, cell body migration was not inhibited. Microinjection of a non-caged phosphorylated tyrosine 397 FAK peptide into migrating NBT-II cells also led to lamellar arrest; however, this approach lacks the temporal control afforded by the caged phosphopeptides. Photoactivation of related phosphotyrosine peptides with altered sequences did not result in transient lamellar arrest. We hypothesize that the phosphorylated FAK peptide competes with the endogenous FAK for binding to FAK effectors including, but not limited to, Src and phosphoinositide 3-kinase, causing spatiotemporal misregulation and subsequent lamellar arrest.

Focal adhesions are cell-surface specializations that connect the extracellular matrix to the actin cytoskeleton. Transmembrane integrins and associated cytoskeletal proteins, including talin, vinculin, α-actinin, and filamin, perform this function within the focal adhesion (1, 2). In addition, focal adhesions contain numerous regulatory molecules, including focal adhesion kinase (FAK),[1] which is a non-receptor tyrosine kinase. Cell binding to the extracellular matrix clusters integrins, which, in turn, stimulates phosphorylation of FAK on tyrosine 397; this creates docking sites where SH2 domain-containing proteins, such as Src, can bind. In this way, FAK links integrin receptors to intracellular signaling events related to cell migration and survival.

The importance of FAK in cell migration was demonstrated when FAK null fibroblasts showed reduced migration compared with wild type cells generated from the same stage of mouse embryos (3). The migration defect could be rescued by expression of wild type FAK (4, 5). Overexpression of FAK in Chinese hamster ovary cells also resulted in increased migration (6). However, neither re-expression of mutated FAK (Y397F) in the FAK null cells nor overexpression of Y397F in Chinese hamster ovary cells enhanced migration. Upon phosphorylation, the region containing tyrosine 397 may bind to the SH2 domains of Src (7, 8), phospholipase C-γ1 (9, 10), phosphatidylinositol 3-kinase (PI3K) (10, 11), Grb7 (12–14), Nck-2 (15), and Shc (16), thus mediating numerous downstream effects. The defect in the stimulation of migration exhibited by Y397F is presumably because of a resultant inability to recruit one or more of these binding partners.

FAK phosphopeptides have been synthesized to test interactions of phosphotyrosine 397 (pTyr^{397} FAK) with the SH2 domains of Src (17) and PI3K, respectively (11). Chen (11) used a FAK Tyr^{397} phosphopeptide to disrupt the binding of the p85 subunit of PI3K to full-length FAK *in vitro* using GST fusion proteins. Peptides containing the pTyr^{397} FAK region of FAK might therefore be useful for probing FAK function in migrating cells. In the present work, we investigated the role of pTyr^{397} FAK within FAK by introducing photoactivatable caged phosphopeptides containing Tyr^{397} and the surrounding sequence into migrating cells.

A caged compound includes a photocleavable protecting group that masks an essential functionality. In this context, a peptide or protein is prepared by covalently linking a photolabile protecting group to a limited number of critical func-

* This work was supported in part by the Cell Migration Consortium (GM64346). The costs of publication of this article were defrayed in part by the payment of page charges. This article must therefore be hereby marked "*advertisement*" in accordance with 18 U.S.C. Section 1734 solely to indicate this fact.

¶ These authors contributed equally to this work.
‖ Recipient of a fellowship from the Lineberger Comprehensive Cancer Center.
‡‡ Recipient of a postdoctoral fellowship from the International Human Frontier Science Program Organization.
§§ To whom correspondence should be addressed. Tel.: 919-966-5703; Fax: 919-966-1856; E-mail: frap@med.unc.edu.

[1] The abbreviations used are: FAK, focal adhesion kinase; SH2, Src homology 2; PI3K, phosphatidylinositol 3-kinase; pTyr, phosphotyrosine; cpTyr, caged pTyr; HPLC, high performance liquid chromatography; GST, glutathione *S*-transferase; HBTU, *O*-benzotriazolyl-*N*-*N*-*N*′-*N*′-tetramethyluronium hexafluorophosphate; HOBt, 1-hydroxybenzotriazole; MS(ESI), mass spectrometry (electrospray ionization); DIEA, *N*,*N*-diisopropylethylamine; DMF, *N*,*N*-dimethylformamide; Ahx, aminohexanoic acid; Fmoc, *N*-(9-fluorenyl)methoxycarbonyl; Rh, rhodamine.

tional groups in the biomolecule (18). The caged peptides can be introduced into the cells by microinjection. Upon removal of the caging moiety by photolysis, the bioactive form of the peptide or protein is produced within the cell (19, 20). Photoactivation of caged proteins/peptides thus offers insights into cellular dynamics not achievable using genetic methods: perturbations that can be controlled temporally and, in some cases, spatially are followed with subsequent observations of altered cell behavior. However, thus far, there are few studies using caged peptides and proteins to study cell migration (21–24).

In this study, we showed that photoactivation of a caged phosphotyrosine peptide (cpTyr^{397}FAK), based on the sequence of FAK from residues Val^{391} to Thr^{406} surrounding the autophosphorylation site at Tyr^{397}, alters cell migration by temporarily halting lamellar extension. The effect on migration is specific for the pTyr^{397}FAK sequence because similar peptides containing phosphotyrosine but with altered surrounding residues fail to alter cell migration upon uncaging. The time scale of temporary inhibition of migration is consistent with the time to dephosphorylate the pTyr^{397}FAK peptide in cell lysates. We speculate that the phenotype is related to perturbation of FAK-effector interactions including, but not limited to, Src and PI3K.

MATERIALS AND METHODS

General Chemical Methods

Peptides containing tyrosine (Tyr), free phosphotyrosine (pTyr), and caged phosphotyrosine (cpTyr) were synthesized using standard Fmoc solid phase peptide synthesis protocols, purified by high performance liquid chromatography (HPLC), and confirmed as the desired products by mass spectrometry. The caged phosphotyrosine residue was incorporated into the peptide sequence using a new building block for solid phase synthesis (25). All peptide synthesis reagents were purchased from Applied Biosystems or Novabiochem, and all other chemicals were purchased from Sigma or Molecular Probes. High performance liquid chromatography was performed using a Waters 600E HPLC fitted with a Waters 600 automated control module and a Waters 2487 dual wavelength absorbance detector recording at 228 and 280 nm. For analytical HPLC a Beckman Ultrasphere C_{18}, 5 μm, 4.6 × 150-mm reverse phase column was used. For preparative separations a YMC-pack, C_{18}, 250 × 20-mm reverse phase column was used. The standard gradient for analytical and preparatory HPLC used was 93:7–0:100 over 35 min (water:acetonitrile, 0.1% trifluoroacetic acid). Electrospray ionization mass spectrometry was performed on a PerSeptive Biosystems Mariner Biospectrometry Workstation (turbo ion source).

Peptide Synthesis—Peptide synthesis was made using standard solid phase peptide synthesis protocols on a 0.05-mmol scale using a 0.21 mmol/g loading PAL-PEG-PS solid support. Amino acids were purchased from Novabiochem as protected Fmoc amino acids with the standard side chain protecting scheme: Fmoc-Ala-OH, Fmoc-Arg(Pbf)-OH, Fmoc-Asp(OtBu)-OH, Fmoc-Glu(OtBu)-OH, Fmoc-Ile-OH, Fmoc-Ser(tBu)-OH, Fmoc-Thr(tBu)-OH, Fmoc-Tyr(tBu)-OH, and Fmoc-Val-OH. Phosphotyrosine was introduced as the monobenzyl ester Fmoc-Tyr(PO(OBzl)OH)-OH.

Amino acids were manually coupled in 4-fold excess using a mixture of *O*-benzotriazolyl-*N*-*N*-*N*′-*N*′-tetramethyluronium hexafluorophosphate (HBTU) and 1-hydroxybenzotriazole (HOBt) and *N*,*N*-diisopropylethylamine (DIEA) in DMF as activating agents. Each amino acid was activated for 2 min with the HBTU/HOBt mixture and DIEA in DMF before being added to the resin. Amide coupling reactions were conducted for 1 h and monitored using the 2,4,6-trinitrobenzenesulphonic acid TNBS test (26). Deprotection of the base-labile Fmoc protecting group was accomplished by treating the resin with 20% piperidine in DMF solution for 15 min. Acetylation was accomplished by treating the resin with acetic anhydride and DIEA in DMF. Peptides were cleaved from the resin, and side chain protecting groups were simultaneously removed by treatment with the following cleavage mixture: 50 μl of dichloromethane, 25 μl of triisopropyl silane, 25 μl of water, and 950 μl of trifluoroacetic acid (1 ml of mixture/50 mg of resin) for 2 h at room temperature. All peptides were precipitated with diethyl ether (4 °C) and further purified by HPLC. Operations involving the caged phosphotyrosine peptides were performed in the dark.

Detailed Protocol for a Typical Coupling—Piperidine (3 ml, 20% in DMF) was added to 0.05 mmol FmocHN-AEIIDEEDT in solid support, and nitrogen was passed through the mixture for 15 min. The resin was then filtered and washed with DMF (3 × 3 ml × 3 min), and the TNBS test was run with a small resin sample to confirm that the deprotection was successful. In a separate vessel, Fmoc-Tyr(tBu)-OH (79 mg, 0.2 mmol) was dissolved in HOBt/HBTU solution (1 ml 0.2 M HBTU, 0.2 M HOBt in DMF), and DIEA (1.5 ml of 0.195 M solution in DMF) was added. The resulting mixture was activated for 2 min and then added to the resin. Nitrogen was passed through the resin suspension for 1 h, at which time the TNBS test of a small resin sample was negative. The resin was washed with DMF (3 × 3 ml × 3 min) and subjected to the subsequent deprotection/coupling cycles in a similar manner.

Acetylation—A 500-μl aliquot of acetic anhydride and DIEA (3 ml, 0.195 M in DMF) were added to the resin-bound free amino-terminal peptide. Nitrogen was passed through the mixture for 15 min. The resin was filtered and washed with DMF (3 × 3 ml × 3 min) and CH_2Cl_2 (2 × 3 ml × 3 min) and dried under vacuum before cleavage.

Cleavage—A 0.05-mmol sample of resin-bound peptide was dried overnight and placed in a 50-ml flask. To this, 5 ml of the cleavage mixture (250 μl of CH_2Cl_2, 125 μl of water, 125 μl of tri-isopropylsilane, trifluoroacetic acid to 5 ml) was added, and the resulting mixture was shaken for 2 h, the resin was filtered, and the trifluoroacetic acid filtrate was concentrated under an argon stream to a volume of 2 ml and added over ice-cold ethyl ether (40 ml). After 5 min, the peptide was centrifuged and washed again with 40 ml of cold ether. The solid residue was dried under argon, redissolved in acetonitrile/water 1:1 (5 ml), and purified by preparative reverse phase HPLC. The pooled fractions were lyophilized and redissolved in deionized water. In some cases, addition of a small amount of base (0.05% $NaHCO_3$) was necessary to solubilize the peptides. The identity of the final peptide products was confirmed by electrospray ionization mass spectrometry.

Coupling with Rhodamine—For rhodamine coupling, a 0.015-mmol aliquot of free amine-containing peptide on solid support was washed with DMF (3 × 3 ml × 3 min) and filtered. The resin was then suspended in DMF (500 μl) and DIEA (50 μl, 0.3 mmol, 20 eq), and to this mixture was added 5 (and 6)-carboxy)-X-rhodamine, succinimidyl ester (12 mg, 0.02 mmol). The resulting mixture was stirred in the dark overnight. The resin was filtered, washed with DMF (3 × 3 ml × 3 min), iPrOH (2 × 3 ml × 3 min), and dichloromethane (3 × 3 ml × 3 min), dried under vacuum, and stored at 4 °C.

Peptide Characterization—Peptides were purified by reverse phase HPLC, and concentrations of stock solutions were determined by quantitative amino acid analysis. When bright chromophores were present (rhodamine), then the reported extinction coefficients for those chromophores were used for calculating the concentrations by spectrophotometry.

cpTyr^{397}FAK sequence: Ac-VSETDD-cpY-AEIIDEEDT-$CONH_2$, $C_{86}H_{125}N_{18}O_{42}P$, Mass.: 2112.8, MS(ESI); 1057.9 ($[MH_2]^{2+}$ (100); 720.3, $[MHNa_2]^{3+}$ (8)), ϵ (M^{-1}, cm^{-1}) 5332 (267 nm).

pTyr^{397}FAK sequence: Ac-VSETDD-pY-AEIIDEEDT-$CONH_2$, $C_{78}H_{118}N_{17}O_{40}P$, Mass.: 1963.7, MS(ESI); 1057.9, $[MH_2]^{2+}$ (100). ϵ (M^{-1}, cm^{-1}) 350 (264 nm).

Rh-Ahx-cpTyr^{397}FAK sequence: Rh-Ahx-VSETDD-cpY-AEIIDEEDT-$CONH_2$, $C_{123}H_{163}N_{21}O_{46}P^+$, Mass.: 2701.1, MS(ESI): 908.3 $[MHNa]^{3+}$ (70), 915.6 $[MNa_2]^{3+}$ (100), 923 $[MNa_3\text{-}H]^{3+}$; ϵ (M^{-1}, cm^{-1}) 80,000 (576 nm).

Rh-Ahx-pTyr^{397}FAK sequence: Rh-Ahx-VSETDD-cpY-AEIIDEEDT-$CONH_2$, $C_{115}H_{156}N_{20}O_{44}P^+$, Mass.: 2552.0, MS(ESI): 866.0 $[MNa_2]^{3+}$ (60), 873.6 $[MNa_3\text{-}H]^{3+}$, (100) 880.6 $[MNa_4\text{-}2H]^{3+}$ (50); ϵ (M^{-1}, cm^{-1}) 80,000 (576 nm).

Rh-Ahx-scrambledFAK sequence: Rh-Ahx-DDVETS-Y-AEIIDEEDT-$CONH_2$, $C_{115}H_{155}N_{20}O_{41}^+$, Mass.: 2472.0, MS(ESI): 1248.0 $[Mna]^{2+}$ (100), 1259.0 $[MNa_2\text{-}H]^{2+}$, (40) 1270.0 $[MNa_3\text{-}2H]^{2+}$ (25); ϵ (M^{-1}, cm^{-1}) 80,000 (576 nm).

Ala^{395}cpTyr^{397}FAK sequence: Ac-VSETAD-cpY-AEIIDEEDT-$CONH_2$, $C_{85}H_{125}N_{18}O_{40}P$, Mass.: 2068.8, characterized before final acetylation: $C_{83}H_{123}N_{18}O_{39}P$, Mass.: 2026.8 MS(ESI); 1014.8 $[MH_2]^{2+}$ (100), 1025.8 $[MHNa]^{2+}$ (20); ϵ (M^{-1}, cm^{-1}) 5332 (267 nm).

Ala^{395}pTyr^{397}FAK sequence: Ac-VSETAD-pY-AEIIDEEDT-$CONH_2$, $C_{77}H_{118}N_{17}O_{38}P$, Mass.: 1919.7, MS(ESI): 982.8 $[MNa_2]^{2+}$ (70), 993.8 $[MNa_3\text{-}H]^{2+}$ (100), 1004.8 $[MNa_4\text{-}2H]^{2+}$ (60), 1015.7 $[MNa_5\text{-}3H]^{2+}$ (30).

Ala^{395}Ala^{396}cpTyr^{397}FAK sequence: Ac-VSETAA-cpY-AEIIDEEDT-$CONH_2$, $C_{76}H_{118}N_{17}O_{36}P$, Mass.: 1875.7, characterized before final acetylation: $C_{82}H_{123}N_{18}O_{37}P$, Mass.: 1982.8 MS(ESI); 992.8 $[MH_2]^{2+}$ (100), 1003.3 $[MHNa]^{2+}$ (25).

Lifetime of pYFAK after Uncaging—A 25-ml sample of NBT-II cell culture was centrifuged; the pellet was then treated with 250 μl of 1% Triton X-100 in phosphate-buffered saline solution and gently mixed with a micropipette. The resulting mixture was transferred to a 1-ml tube and centrifuged at high speed (13,000 rpm) for 8 min. An 80-μl

aliquot of the supernatant was added to 5.6 μl of *Rh-Ahx-pYFAK* stock solution (30.5 μM) to give a final peptide concentration of 2 μM. The resulting mixture was incubated at 25 °C, and 3-μl aliquots were taken consecutively at 5, 10, 15, 20, and 25 min and diluted in 100 μl of phosphate-buffered saline, pH 7.5. Each sample was kept frozen at −78 °C until injected into the HPLC for analysis.

As a control, an 80-μl aliquot of lysate was treated for 5 min with 400 μM pervanadate to inactivate tyrosine phosphatases, and then 5.6 μl of stock *Rh-Ahx-pYFAK* solution was added to the lysate and the peptide was incubated at room temperature. For analysis, 3-μl aliquots were taken at 10 and 20 min and added to 100 μl of phosphate-buffered saline, pH 7.5. Each sample was kept frozen at −78 °C until injection onto the HPLC for analysis. 160 μl of NBT-II cell lysate (from 20 ml of culture) was incubated with Flu-pYFAK (final concentration 2 μM).

GST·Src SH2 and GST·PI3K C-terminal SH2 Expression and Purification—Src and PI3K SH2 domains were expressed and purified as GST fusion proteins essentially following reported procedures (27). In summary, plasmids encoding the GST fusion proteins were transformed into bacteria *Escherichia coli* DH5-competent cells; Invitrogen). Bacteria were grown to mid-log phase, induced at 37 °C for 3–4 h with isopropyl-1-thio-β-D-galactopyranoside, and lysed by treatment with lysozyme (1 mg/ml, 30 min) followed by sonication (phosphate-buffered saline buffer, pH 7.4, with 100 mM EDTA, 1% Triton X-100, 10% glycerol, 1 mM dithiothreitol, 0.1 mM 4-(2-aminoethyl)benzenesulfonyl fluoride (AEBSF), 30 μg/ml leupeptin, and 0.5 μg/ml pepstatin A). The lysates were clarified by centrifugation, and fusion proteins were purified by binding to glutathione-agarose beads (Amersham Biosciences). Proteins were eluted from the beads (50 mM Tris-HCl, 10 mM reduced glutathione, pH 8) and concentrated by centrifugation through a cellulose membrane (10 kDa molecular mass cutoff; Millipore). Proteins were quantified by Micro BCA protein assay kit (Pierce) relative to a bovine serum albumin standard. All fusion proteins were analyzed by Coomassie Blue staining and Western blot analysis with anti-GST antibodies.

K_d Values for Peptide Binding to SH2 Domains of Src and PI3K—All experiments were performed using a VP-ITC instrument from Microcal Inc. Peptides and proteins were dialyzed extensively against the same buffer (50 mM Tris-HCl, pH 7.4, 100 mM NaCl, 1 mM β-mercaptoethanol) using a 500-Da molecular mass cutoff cellulose membrane (Spectrum Laboratories Inc.). Initial experiments using lower pH resulted in precipitation of the protein and/or peptide during the titration.

In a typical titration, peptides (1–3 mM concentration) were added over 25 injections (5 μl) to purified GST·SH2 proteins (200–400 μM) that were present in the isothermal calorimeter cell at 25 °C. This temperature was chosen to minimize the contributions of ligand-induced refolding of the protein while maintaining a physiologically relevant temperature of operation. In every titration the concentration of the reactants was sufficient to result in saturation of the titration curve.

Biological Methods

Cell Culture—For the movement of NBT-II cells, suspension culture Petri dishes (35 mm) were coated by incubating with 10 μg/ml collagen (rat tail type I) for 30 min. NBT-II cells (American Type Culture Collection) were treated with trypsin and resuspended in Dulbecco's modified Eagle's medium/F12 medium containing 10% fetal bovine serum, plated at low density on the dishes, and cultured for 12 h at 37 °C.

Competitive Binding Assay in Cell Lysates—As previously described, chicken embryo cells were isolated from day 9 embryos and maintained in Dulbecco's modified Eagle's medium + 4% fetal bovine serum + 1% chick serum (28). FAK was expressed in chicken embryo cells using the replication-competent, avian retroviral vector called RCAS, and cells were transfected as previously described (28, 29). Cells were lysed in modified radioimmune precipitation assay buffer (30) containing protease and phosphatase inhibitors as described (30). The protein concentration of lysates was determined by using the bicinchonic acid assay (Pierce). The expression of GST fusion proteins (Src or PI3K SH2 domains) was induced by using 0.1 mM isopropyl-1-thio-β-D-galactopyranoside. *E. coli* were harvested, lysed by sonication, and the fusion proteins purified by using glutathione-agarose beads (Sigma) as previously described (30).

GST pulldowns were performed from 0.2 mg of lysate from chicken embryo cells expressing FAK. Lysates were precleared with 10 μg of GST. The supernatant was then incubated with 10 μg of fusion protein immobilized on glutathione-agarose beads either with or without peptides at increasing concentrations for 1 h at 4 °C. The beads were washed twice with lysis buffer and twice with phosphate-buffered saline. Bound proteins were eluted by boiling in sample buffer (31) and analyzed by Western blotting with polyclonal antiserum BC4 to recognize FAK. Western blots were incubated with horseradish peroxidase-conjugated secondary antibodies and processed for enhanced chemiluminescence (Amersham Biosciences).

Microinjection—Microinjection of peptides into cells was performed with a semiautomatic Eppendorf InjectMan NI 2/Femtojet system. Original Eppendorf Femtotip needles were loaded with 1.5–2 μl of injection solution. The base pressure of the system was adjusted (by visual assessment of the fluorescent marker outflow from the microinjection needle in the 20–100 hectopascal range) to keep a constant low outflow of the loaded solute into cell medium. Similarly, because of the increasing viscosity of the loaded solution, the injection pressure was adjusted to achieve a similar brightness of co-loaded fluorescent marker in microinjected cells (50 to up to 1200 hectopascal in some cases). After setting up the vertical limit position of the microneedle, each cell was automatically injected with peptide solution by InjectMan with preset speed of the microinjection needle movement. The velocity of the microneedle movement varied from 45 to 130 μm/s. The procedure was repeated to obtain the desired number of microinjected cells. Cells microinjected with caged phosphopeptides were allowed to recover in the tissue culture incubator for 30 min. During microinjection and subsequent time lapse microscopy, cells were maintained at 37 °C and CO_2 was flushed over the dish. To distinguish between microinjected and non-microinjected cells, a tracer (either rhodamine-labeled peptide or rhodamine-dextran) was co-loaded with the peptides at a final concentration range <10% of that of biological test peptide.

We evaluated the consistency of microinjected volumes when different caged peptides were introduced. NBT-II cells, seeded on glass or plastic surface, were microinjected with either cpTyr^{397}FAK or Ala^{395}cpTyr^{397}FAK peptides together with fluorescent marker (rhodamine dextran) as described above. Cells were left in the incubator for 1 h and then placed in an environmental chamber on the microscope stage. From phase contrast and epifluorescence images of cells loaded with rhodamine dextran, the area of cells of interest was manually outlined and the average value of fluorescence of the outlined area was determined using Metamorph imaging software routines. The mean value (arbitrary units) of single cell average fluorescence was 105 ± 27 for cpTyr^{397}FAK (269 cells) and 97 ± 28 for Ala^{395}cpTyr^{397}FAK (143 cells). The results indicated that constant volumes of the solutions containing cpTyr^{397}FAK or Ala^{395}cpTyr^{397}FAK peptides could be microinjected.

Photoactivation—For uncaging of caged FAK phosphopeptides, UV light from an Argon ion laser (Spectra Physics), with multiline optics covering a 333.6–363.8-nm range, was focused onto a ~8-μm-diameter spot on the specimen using a ×20 Nikon objective. For all experiments, the estimated power of the laser beam after passing through the objective was 67 microwatts (measured by a power meter) and the duration of illumination was 100 ms.

Concentration Estimates of Microinjected and Uncaged Peptide—Estimates for the concentration of the microinjected peptides as well as uncaged peptide are given in Table I. Using the Eppendorf Injectman, we estimate that 20–200 fl of peptide is microinjected into each cell. If the average cell volume of NBT-II cells is 1.5 pl, an additional 1–10% (32) of the total cell volume is added by microinjection. To estimate the concentrations of peptide after uncaging, a quantum efficiency of uncaging for these peptides of 0.3 was used based on characterization of a paxillin peptide with the same caging moiety (33).

Microscopy and Cell Motility Measurements—Cell migration was measured with a Nikon Diaphot 300 microscope using ×20 Phase 3 DL 0.75 N.A. objective. The microscope was equipped with a Cooke Sensicam QE CCD camera and a semiclosed perfusion microincubator (Harvard Apparatus). The temperature of the chamber was kept at 37 °C, and CO_2 flow was maintained over the Petri dish. Time lapse images of migrating cells were taken between 1–4 h; images were recorded every 5 min. The movement of individual cells was analyzed with Metamorph software (Universal Imaging).

RESULTS

Characterization of Peptide Properties

Peptides Employed—The series of peptides synthesized for this study is shown in Fig. 1, and the rationale for their design is given under "Discussion." The peptides are based on the sequence of FAK from residues Val^{391} to Thr^{406} surrounding the autophosphorylation site at Tyr^{397} (VSETDD-pY^{397}AEIIDEEDT) (pTyr^{397}FAK); a closely related peptide (VSETDDY^{397}AEIIDEED) has been previously used in studies to inhibit Src SH3-SH2/phosphoprotein interactions in a com-

TABLE I
Estimated concentration of microinjected and uncaged peptide

Peptide	Concentration of peptide in microinjection needle	Peptide concentration in cell after microinjection[a]	Concentration uncaged (lower limit)[b]
		μM	
pTyr^{397}FAK	977 μM	10–100	NA[c]
	195 μM	2–20	NA[c]
	98 μM	1–10	NA[c]
cpTyr^{397}FAK	930 μM	9–90	2.7–27
Ala^{395}cpTyr^{397}FAK	1.394 mM	14–140	4–40
Ala^{395}pTyr^{397}FAK	3.17 mM	32–320	NA[c]
	370 μM	3–30	NA[c]
Ala^{395}Ala^{396}cpTyr^{397}FAK	1.232 mM	12–120	3.6–36
Partially scrambled FAK	513 μM	5–50	NA[c]

[a] The amount microinjected is based on microinjecting 1–10% of total cell volume (28) and an estimated NBT cell volume of 1.5 pl.
[b] The lower limit estimate of uncaged peptide is based on the quantum efficiency of peptide uncaging (0.3 *in vitro*) (29) and complete uncaging in a cylindrical volume ~9 μm in diameter and ~4 μm high during the 100-ms irradiation time. Some diffusion of caged peptide into the irradiation zone during the irradiation will increase the amount of peptide uncaged.
[c] NA, not applicable.

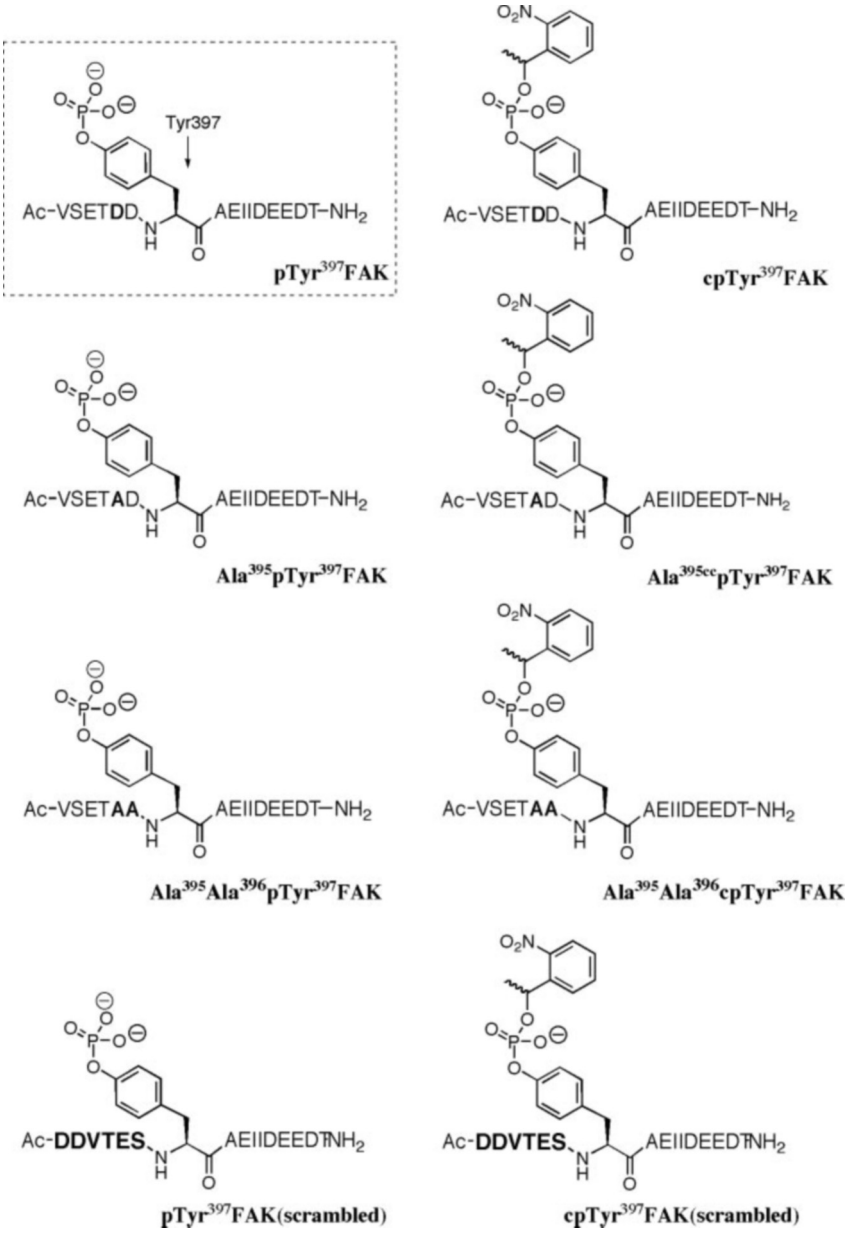

FIG. 1. **Peptides employed in this study.** See "Results" for description.

petition enzyme-linked immunosorbent assay (34). For photoactivation, a caged phosphotyrosine (cpY, or cpTyr) was introduced into the sequence (VSETDDcpY^{397}AEIIDEEDT) designated cpTyr^{397}FAK. In addition, a similar caged phosphotyrosine peptide with an amino acid substitution at position 395 (alanine for aspartic acid) was synthesized (VSETADcpY^{397}AEIIDEEDT) and designated Ala^{395}cpTyr^{397}FAK. A caged phosphotyrosine-containing peptide with 2 amino acid substitutions (D395/396A) (VSET-

TABLE II
Dissociation constants for peptide binding to GST·SH2 motifs of Src and N-terminal p85 of PI3K

Peptide	K_d binding to Src SH2	K_d binding to N-terminal p85 SH2 of PI3K
	μM	
pTyr^{397}FAK	3.7 ± 1.5	47 ± 12
Ala^{395}pTyr^{397}FAK	4.7 ± 0.8	54 ± 13
Partially scrambled pyFAK	3.5 ± 1.6	46 ± 18

AAcpY^{397}AEIIDEEDT), designated Ala^{395}Ala^{396}cpTyr^{397}FAK, and another non-caged peptide with amino acid sequence N-terminal of the phosphotyrosine shuffled (AcDDVTESpY^{397}AEIIDEEDT), designated partially scrambled pYFAK, were also synthesized.

K_d Values for Peptide Binding to SH2 Domains of Src and PI3K—As likely targets for peptide binding are Src and PI3K, we determined the binding affinities of several of the phosphopeptides to GST fusions of Src and PI3K SH2 domains using isothermal titration calorimetry (Table II). Dissociation constants for pTyr^{397}FAK, Ala^{395}pTyr^{397}FAK, and partially scrambled pTyr FAK binding to Src SH2 domains are similar at about 4 μM. Current models for binding of similar peptides to Src SH2 motifs place emphasis on the pYAEI sequence C-terminal to Tyr^{397} in FAK as the major determinant of binding. In addition, all peptides tested bind more strongly to Src as compared with PI3K SH2 motifs with K_ds that are about one order of magnitude lower.

Competitive Binding Assay in Cell Lysates—The results in Fig. 2 show that in cell lysates, pTyr^{397}FAK is able to compete for FAK binding to the Src SH2 domain in the μM range. Surprisingly, the Ala^{395}pTyr^{397}FAK peptide competes even more effectively for FAK binding to the Src SH2 domain. Both peptides compete for FAK-PI3K binding in the 10–50-μM range, and the Ala^{395}pTyr^{397}FAK competes better than the wild type peptide. The lysate competition assay results and the isothermal calorimetry determination of K_ds of various peptide bindings to purified SH2 domains from PI3K and Src are qualitatively consistent. However, the data from these two measurements show the Ala^{395}pTyr^{397}FAK peptide is not defective for binding to PI3K, contrary to predictions based on literature precedent (35).

Lifetime of pTyr^{397}FAK in Cell Lysates after Uncaging—After microinjection of the pTyr^{397}FAK peptide or uncaging of the cpTyr^{397}FAK peptide, the most likely mode of degradation is via dephosphorylation by endogenous phosphatases. Because this action would deactivate the peptide reagent, it was important to estimate the kinetics of dephosphorylation of the intact phosphopeptide. Using HPLC analysis, the dephosphorylation of the FAK phosphopeptides in NBT-II cell lysates was followed at 25 °C (Fig. 3). Aliquots of NBT-II cell lysates incubated with Rh-pTyr^{397}FAK peptide were taken every 5 min and analyzed by HPLC using rhodamine fluorescence for monitoring. We observed the formation of a new product with retention time that matches that of the Rh-Tyr^{397}FAK sample (Fig. 3*A*). The resulting chromatograms show a steady decrease in the peak corresponding to the phosphopeptide and a simultaneous increase in the intensity of another fluorescent peak with the same retention time as the unphosphorylated peptide. From the HPLC traces, we conclude that the half-life of the phosphopeptide in the NBT-II cell lysates is 10–15 min, in agreement with reported literature values (34). As expected, incubation of the peptide with pervanadate-treated cell lysates does not show degradation of the peptide during the time of the experiment, suggesting that the change in retention time of the peptide was due to dephosphorylation by tyrosine phosphatases in the lysate (Fig. 3*B*). Over a similar time frame, the caging group protects the phosphate group from phosphatase-mediated degradation (see Fig. 3*C*).

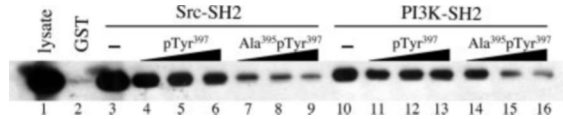

FIG. 2. **Ability of phosphorylated FAK peptides to compete for binding to Src and PI3K SH2 domains.** The Src and PI3K SH2 domains were expressed as GST fusion proteins and immobilized to glutathione-agarose beads. FAK-expressing chicken embryo cell lysate was precleared by incubation with GST alone immobilized to glutathione-agarose beads. The cleared lysates were then incubated with GST (*lane 2*), GST·Src SH2 (*lanes 3–9*), or GST·PI3K SH2 (*lanes 10–16*). Pulldowns were also performed in the presence of the wild type pTyr^{397}FAK peptide or the Ala^{395}pTyr^{397}FAK peptide at concentrations of 2 μM (*lanes 4*, *7*, *11*, *14*), 5 μM (*lanes 5*, *8*, *12*, *15*), or 45 μM (*lanes 6*, *9*, *13*, *16*). The beads were washed, and bound FAK was detected by Western blotting. 25 μg of lysate was run as a control (*lane 1*).

Effects of Peptides on Cell Migration

Uncaging of FAK 397 Phosphopeptides Produces a Transient Arrest of Lamellar Extension—NBT-II cells were microinjected with caged phosphopeptides and a tracer (see "Materials and Methods") and then allowed to recover in a 37 °C incubator with 5% CO_2 for 30 min. After recovery, microinjected cells were tracked to ensure there were no migration differences attributable to microinjection. The phosphopeptides were uncaged by two brief flashes of UV laser light (one directed at the lamella and the second on the main cell body (see *blue circles* representing the irradiation spots in Fig. 4*B*; spots drawn to scale). Typical results are given in Fig. 4. The top panel (Fig. 4*A*) shows that migration is normal after cells have recovered from microinjection of cpTyr^{397}FAK. After uncaging, the lamella of the photoactivated NBT-II cells ceased to extend for 20–40 min (Fig. 4*B*, *red line*). During this time, there was little or no change in the morphology of the lamellipodium, suggesting a temporary increase in adherence to the substrate. The lamella stopped protruding within the first minute after photoactivation. Note, however, that the trailing edge of the cell continued to move forward (*green line* indicates the initial position of cell body). In Fig. 4*C*, non-loaded cells were also irradiated to serve as controls for nonspecific photodamage. Under these conditions, these cells continued to migrate at the same rate as before irradiation.

Distribution of lamellar arrest duration in different cells is given in Fig. 5*A*. In these experiments, 18 of 25 cells displayed transient lamellar arrest after photoactivation of cpTyr^{397}FAK (2 cells showed no effect; 4 cells were difficult to assess; 1 cell slowed but did not stop) (Fig. 5*A*). Two laser shots were required to achieve the effect, including one over the perinuclear region. A single irradiation focus on the lamellipod was insufficient. This suggests that this migration "phenotype" is a global effect in the sense that sufficient free phosphopeptide must be released for an effect, and this is provided by the larger volume of uncaging when the beam is directed over the perinuclear zone as opposed to positioning the beam over the much thinner lamella area.

Uncaging Other Peptides—The Ala^{395}cpTyr^{397}FAK peptide (Fig. 1) contains an amino acid substitution in position 395 of the FAK sequence (D395A) that causes full-length FAK mutants to bind to Src but not to PI3K (35). NBT-II cells were microinjected following the procedure used for the caged pTyr^{397}FAK peptides. When the Ala^{395}cpTyr^{397}FAK was uncaged, little lamellar arrest was seen (Fig. 5*B*). Of 20 cells, 14 showed no lamellipodial arrest, 4 temporarily ceased protrusion (2 cells for 15 min, 1 cell for 10 min, and 1 cell for 5 min),

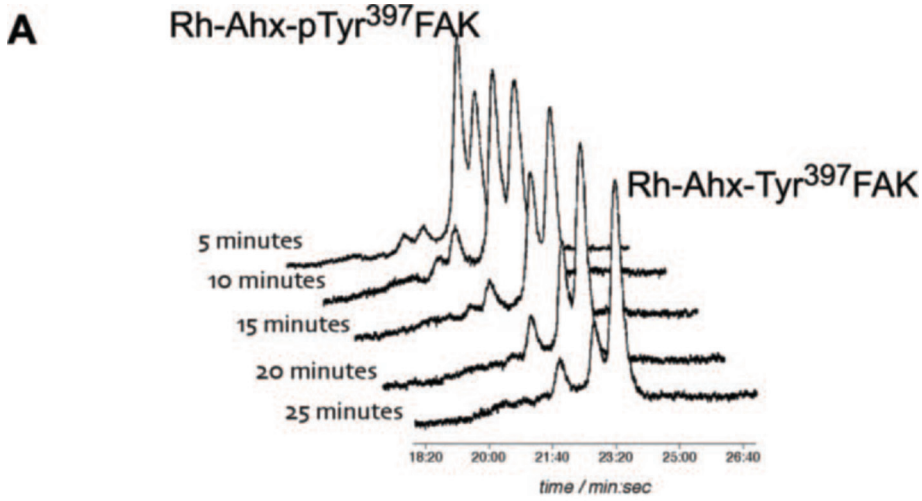

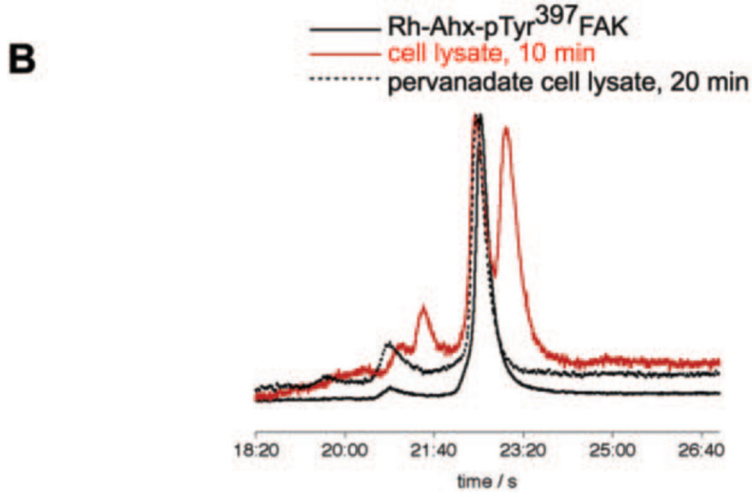

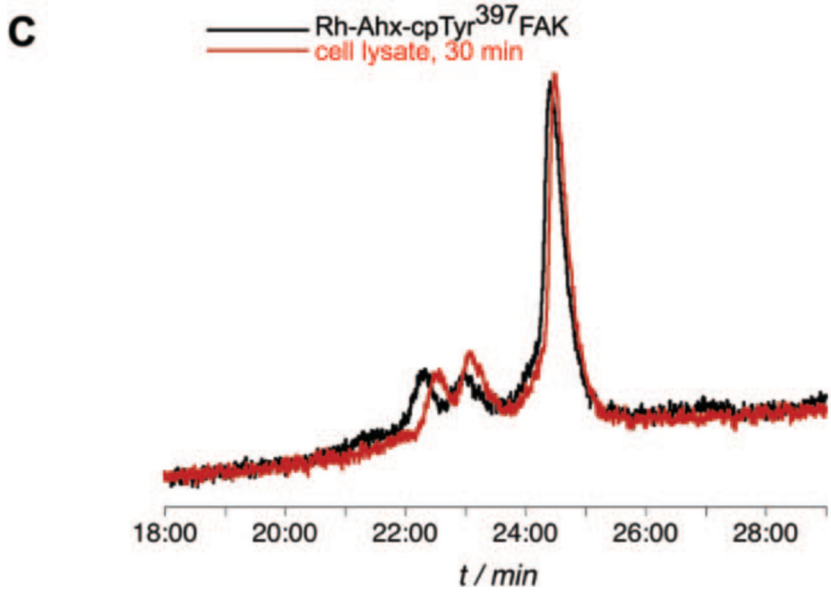

FIG. 3. *A*, HPLC traces of Rh-Ahx-pTyr^{397}FAK (Ahx; 6-aminohexanoic acid linker) incubated with NBT-II cell lysate at 5, 10, 15, 20, and 25 min showing the increase of unphosphorylated peptide. *B*, superposition of the HPLC traces of the stock of Rh-Ahx-pTyr^{397}FAK and the peptide after 20 min of incubation with pervanadate-treated cell lysate, showing that the peptide is stable. *C*, stability of caged phosphopeptide (Rh-Ahx-cpTyr^{397}FAK) in cell lysates.

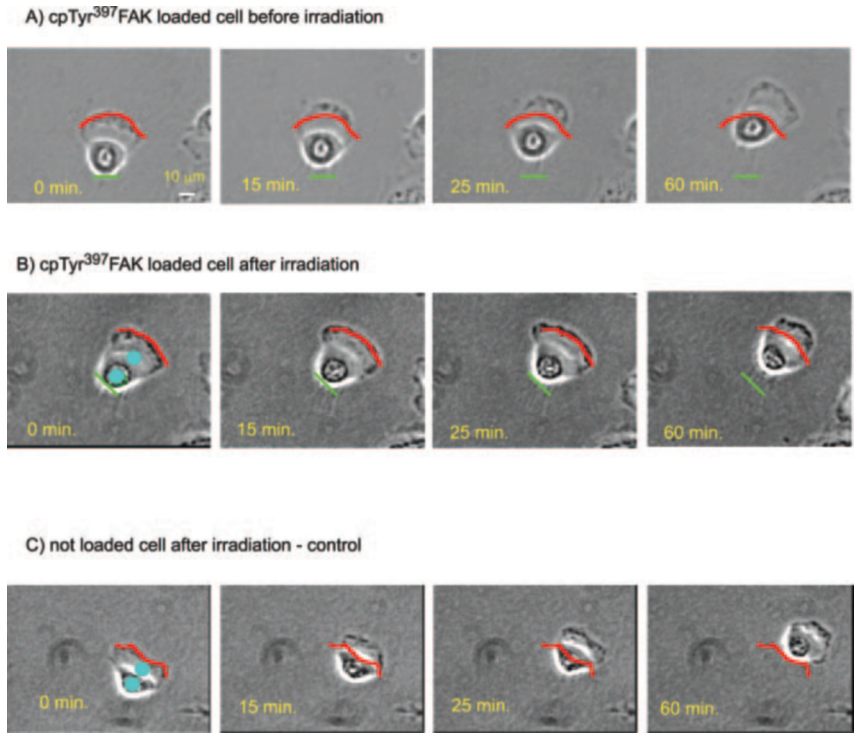

FIG. 4. **Uncaging of cpTyr^{397}FAK peptide produces transient lamellar arrest.** The *red line* indicates the initial position of the leading edge, the *green reference line* indicates the initial position of the trailing edge, and the *blue circles* indicate the regions of irradiation (to scale). *A*, the *top panel* shows a single migrating cell loaded with cpTyr^{397}FAK before laser irradiation. *B*, after photoactivation in *spots shown in circles* (see "Materials and Methods" for details), the release of the phosphopeptide temporarily halts lamellipodial protrusion for 25 min, after which migration resumes. The posterior cell body continues to move forward after peptide photorelease (see *green reference line*), and the lamellipodium broadens before migration continues. *C*, the *bottom panel* depicts a non-loaded, irradiation control showing normal migration after two 100-ms laser irradiations in the spots shown.

and 2 cells were difficult to classify. However, when Ala^{395}pTyr^{397}FAK was directly introduced by microinjection, producing a significantly higher concentration of phosphotyrosine peptide, transient lamellar arrest did occur (see below).

A caged FAK phosphotyrosine peptide containing 2 amino acid substitutions in positions 395 and 396 of the FAK sequence (Ala^{395}Ala^{396}cpTyr^{397}FAK) was designed as a control peptide for uncaging based on the fact that full-length FAK mutants containing the same substitutions have much reduced binding to Src and PI3K (35). Upon photoactivation, most microinjected cells exhibited no appreciable changes in migration speed (results summarized in Fig. 5*C*). These experiments demonstrate the specificity of the peptide sequence required to halt cell protrusion and eliminate the possibility that the effects of uncaging cpTyr^{397}FAK are due to the nitrosoacetophenone side product liberated by photoactivation.

Microinjection of pY^{397}FAK Phosphopeptides Also Produces Transient Lamellar Arrest—Corroborating the contention that uncaging within the lamella cannot release sufficient peptide for an effect is the experiment that directly microinjecting pTyr^{397}FAK peptide produces a similar phenotype (Fig. 6). The pTyr^{397}FAK-loaded NBT-II cell exhibits a temporary inhibition of protrusion before starting to extend small local protrusions between 20–30 min after microinjection and then resumes migration at 45 min. Intermediate concentrations (5–10-fold dilution; ~200 μM in the needle) of pTyr^{397}FAK peptide were required to produce the same effect as uncaging cpTyr^{397}FAK. Microinjection of undiluted pTyr^{397}FAK peptide (~1 mM in the needle) stops migration, and the cells do not recover for the duration of the experiment (1–2 h). This experiment also indicates that the lamellar arrest phenotype is due to the phosphotyrosine peptide itself and not the side product produced after liberation of the caging group. In the pTyr^{397}FAK experiments, described in Fig. 6, changes in the migration rate could be because of either microinjection or peptide. These two possibilities were distinguished by cell morphology. NBT-II cells that have been damaged by microinjection no longer exhibited the fan-like lamellar morphology of a normally migrating cell. Instead, they became rounded and eventually collapsed. In Fig. 6, the microinjected cell maintained its leading lamella and migration resumed after 45 min, indicating that the altered migration was because of the phosphotyrosine peptide and not the microinjection itself.

Caged and free Ala^{395}pTyr^{397}FAK (Fig. 1) were also microinjected into migrating NBT-II cells. Although photoactivation of the caged version of this peptide did not alter migration (Fig. 4*B*), direct microinjection of Ala^{395}pTyr^{397}FAK caused temporary lamellar arrest in 10 of 14 cells (3 cells changed direction, 1 cell showed no arrest). However, microinjection of the partially scrambled FAK phosphopeptide (Fig. 1) did not alter cell migration significantly (9 cells exhibited no noticeable changes, 4 cells changed direction but continued migrating). A summary of the peptide effects on cell migration together with their binding constants to Src and PI3K SH2 motifs and estimated intracellular concentrations is given in Table III.

DISCUSSION

Design of Caged Phosphotyrosine Peptides—Phosphotyrosine peptides containing the amino acids surrounding and including pTyr^{397}FAK have been used previously to study SH2 binding domains of PI3K and Src (11, 17, 34, 36–38). This region of FAK is known to interact not only with the SH2 domains of Src and PI3K but also with SH2 motifs in phospholipase C-γ, SHC, Nck2, and Grb7 (10, 12, 15, 16). Chen *et al.* (11) utilized a 12-amino acid phosphotyrosine peptide to disrupt FAK binding to PI3K (GST-tagged p85 N-terminal SH2 domain) (K_d ~ 10 μM) and to Src (GST-tagged Src-SH2) (K_d ~ 3 μM). These experiments showed that binding of the phosphotyrosine peptide to the p85 subunit of PI3K increased PI3K activity in cell lysates. Other studies also demonstrated the ability of similar phosphotyrosine peptides derived from FAK to activate c-Src (17) and PI3K (39–42). Phosphopeptides that bind Src-SH2 with higher affinity than the Src autoregulatory sequence induce the open, active conformation of the enzyme. Similarly, binding of phosphopeptide to the SH2 domain of p85 (regulatory) subunit of PI3K releases the auto-inhibitory effect permitting catalytic activity of p110 subunit. All of these studies

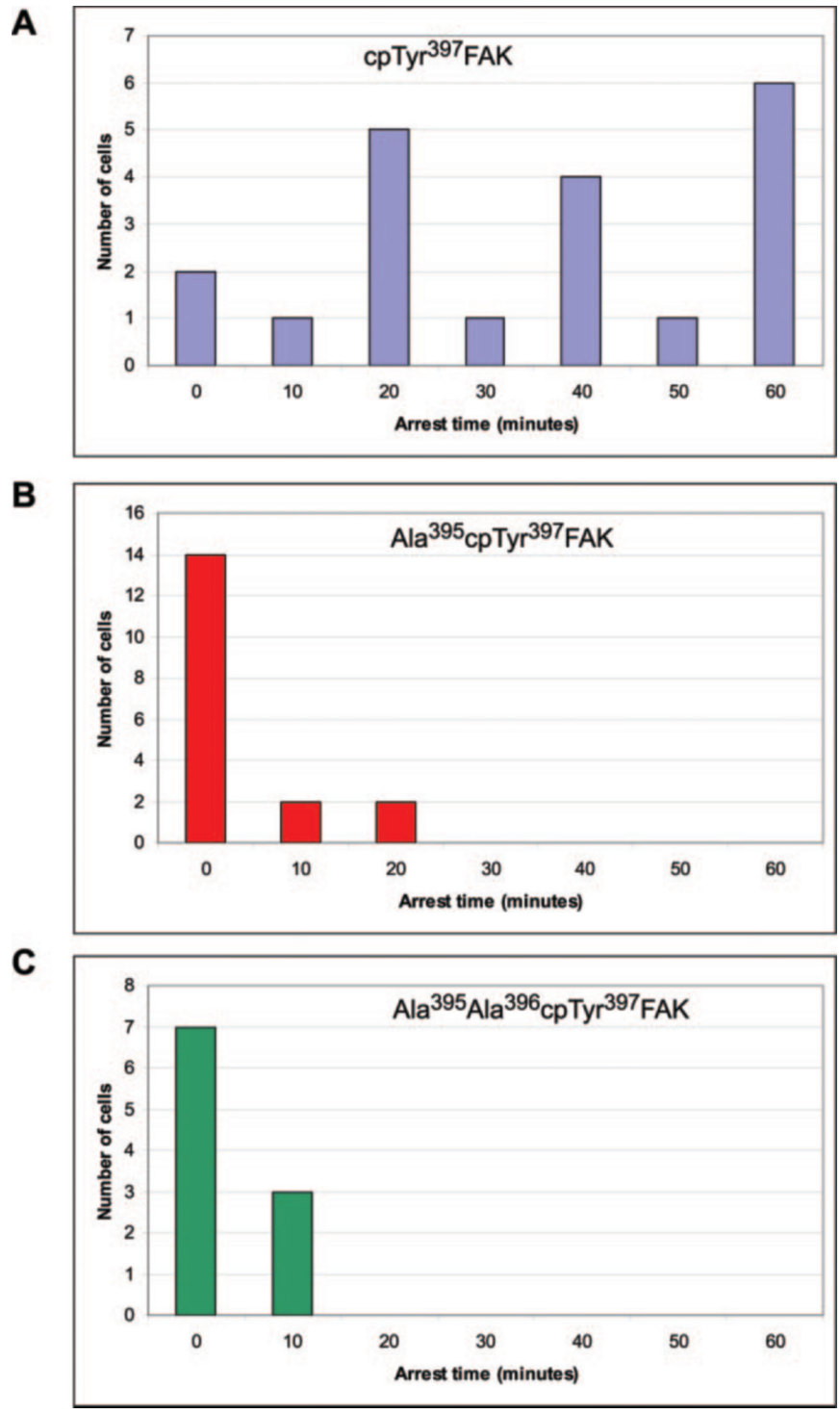

FIG. 5. **Distribution of lamellar arrest durations produced by uncaging cpTyr^{397}FAK (*A*), Ala^{395}cpTyr^{397}FAK (*B*), and Ala^{395}Ala^{396}cpTyr^{397}FAK (*C*).**

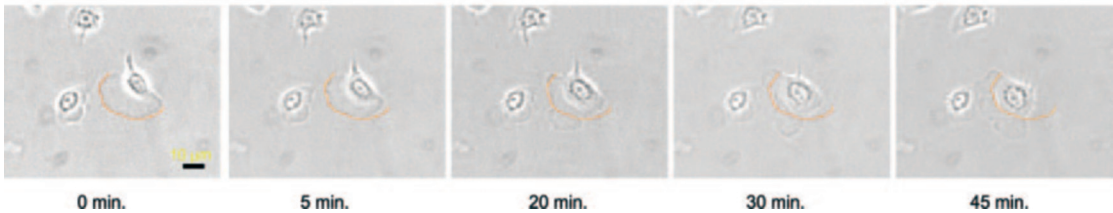

FIG. 6. **NBT-II cells after microinjection with pTyr^{397}FAK peptide.** The time points refer to time elapsed after microinjection. The *red line* indicates the initial position of the leading lamellar edge. The cell stops protruding after microinjection. Between 20–30 min, the cell begins to form two small extensions at different regions of the cell. By 45 min, the cell recovers, shows broad lamellipodial extension, and resumes migration.

TABLE III
Synopsis of peptide effects on cell migration

Peptide	Binding (ITC) K_d[a]		Estimated concentration of microinjected peptide[b]	Estimated concentration of photoactivated peptide	Effect on cell migration
	Src	PI3K			
			μM		
VSETDDcpYAEIIDEEDT (cpTyr^{397}FAK)			9–90	2.7–27	Temporarily halts lamellar protrusion
VSETDDpYAEIIDEEDT (pTyr^{397}FAK) (microinjection only)	3.7	47	2–20	NA[c]	Temporarily halts lamellar protrusion
VSETADcpYAEIIDEEDT (Ala^{395}cpTyr^{397}FAK)			14–140	4–40	No effect on migration
VSETADpYAEIIDEEDT (Ala^{395}pTyr^{397}FAK) (microinjection only)	4.7	54	3–30	NA[c]	Temporarily halts lamellar protrusion
VSETAAcpYAEIIDEEDT (Ala^{395}Ala^{396}cpTyr^{397}FAK)	ND[d]	ND[d]	12–120	3.6–36	Does not affect migration
DDVTESpYAEIIDEEDT (partially scrambled FAK) (microinjection only)	3.5	46	5–50	NA[c]	No effect on migration

[a] From Table II.
[b] From Table I.
[c] NA, not applicable.
[d] ND, not determined.

suggest that the phosphotyrosine peptides such as pYTyr^{397}FAK and cpTyr^{397}FAK could be used as probes inside living cells.

Besides the pYTyr^{397}FAK and cpTyr^{397}FAK peptides, additional phosphotyrosine peptides and their caged counterparts were synthesized as probes and controls (Fig. 1) based on the following rationale. A full-length FAK mutant containing the D395A substitution (2 amino acids upstream from the phosphotyrosine) binds Src, but not PI3K (35). Further, analysis of the consensus PI3K SH2 domain binding motif and structural studies support the role of residues N-terminal to the phosphotyrosine in PI3K binding (37, 38). Therefore, peptides with altered sequences upstream of the phosphotyrosine were designed. These include the Ala^{395}cpTyr^{397}FAK peptide, mimicking the D395A FAK mutant (35), the Ala^{395}Ala^{396}cpTyr^{397}FAK peptide, which contains two substitutions that disrupt the interaction between FAK and both Src and PI3K (35), and a partially scrambled FAK phosphotyrosine peptide with amino acids N-terminal to the phosphotyrosine scrambled (corresponding to FAK 391–396). While these peptides were designed to test the *in vivo* role of amino acids N-terminal to the phosphotyrosine and to distinguish between interactions with Src and PI3K, the isothermal titration calorimetry and lysate competition assays show that the Ala^{395}pTyr^{397}FAK peptide binds to both the Src and PI3K SH2 domains. Thus, different results were obtained with the synthetic mutant peptides and mutants of the full-length protein (35), presumably reflecting additional features of full-length FAK, Src, and/or PI3K that contribute to the stability of the interaction. Although the peptides could not discriminate between effects upon Src and PI3K *in vivo*, the results do demonstrate that sequences N-terminal to the phosphorylated tyrosine play an important role in the observed biological responses.

Selected peptides were caged at the key phosphotyrosine residue using recently developed methodology (25). 1-(2-Nitrophenyl)ethyl (NPE) was chosen as the caging group because it satisfies key requirements of biologically useful caging groups and those of Fmoc-based solid phase peptide synthesis (19, 33). The NPE can be photochemically released with reasonable quantum efficiency at wavelengths around 350 nm (33, 43), and the photo-byproduct, nitrosoacetophenone, is less harmful to cells than the corresponding aldehyde released by photolysis of commonly implemented *o*-nitrobenzyl caging groups (25).

Properties of the Uncaged Peptides—The phosphorylated peptides have a half-life in cell lysates of 10–15 min, roughly consistent with lamellar arrest times. This half-life is only an estimate of stability in intact cells. Isothermal calorimetry studies determining the affinities for the phosphorylated peptides binding to the SH2 domains of Src and PI3K differ by about an order of magnitude, with binding to Src being tighter. These values approximate those reported previously, and any differences in the values probably arise from slight differences in peptide sequences and different methods used to determine affinities (44). Results from the lysate competitive binding assays (Fig. 2) were qualitatively consistent with the isothermal calorimetry data.

Mechanism of Action of the pYFAK Peptides—These phosphotyrosine peptides intervene in signal transduction-mediated events downstream of FAK by abruptly increasing the concentration of pTyr^{397}FAK either upon photoactivation or microinjection to produce transient lamellar arrest. Indeed, this phenotype is remarkably similar to that seen when keratocytes are treated with function-blocking anti-β1 integrin antibodies (45), suggesting that the uncaged peptide intervenes in integrin-mediated signaling pathways. For photoactivation, it appears that in order to liberate sufficient phosphopeptide for an effect, irradiation of the thicker part of the cell was required. Free phosphopeptide then presumably diffuses rapidly throughout the cell and binds to the cognate targets. This view was corroborated by the observation that direct microinjection of intermediate concentrations of phosphopeptides produced a similar transient lamellar arrest phenotype (Fig. 6). Thus, in this case, although temporally defined effects were produced, localized effects could not be created by photoactivation. A similar effect was observed by Walker *et al.* (21) who demonstrated that local photorelease of caged peptide inhibitors of calmodulin or myosin light chain kinase did not produce arrest of eosinophil migration, but global release over the entire cell (similar to microinjection) did. On the other hand, local photorelease of caged actin-binding proteins did produce dramatic local perturbations in migration (22, 24) presumably because a sufficient number of released proteins quickly found their abundant G- or F-actin targets via diffusional encounters.

Two of the most widely studied FAK-binding proteins are Src and PI3K, and previous work has indicated the importance of these two proteins for migration in many cell types (46–49). Our binding and competitive inhibition studies indicate that uncaged peptide could bind to both of these FAK effectors. The literature cited above indicates that similar peptides can activate both Src and PI3K. Thus, temporally and spatially inappropriate activation produces lamellar arrest until the phosphopeptide loses activity via dephosphorylation, at which time normal migration resumes. This does not appear to be the whole story, however. Comparing the actual uncaging results

from cells with the lysate competition results suggests that other FAK effectors such as Shc, PLC-γ, Grb7, or Nck2 may also play a role. Although uncaging of cpTyr^{397}FAK produced the lamellar arrest phenotype, uncaging of Ala^{395}cpTyr^{397}FAK did not; however, the direct microinjection of Ala^{395}pTyr^{397}FAK did produce arrest. This suggests that at the higher microinjected concentrations, Ala^{395}pTyr^{397}FAK most likely titrates other important FAK-effector interactions that are available to uncaged cpTyr^{397}FAK. Further downstream effects that produce this distinctive phenotype remain to be elucidated. These could include 1) an increase in lamellum adhesion or 2) the abrogation of lamellar protrusion by indirectly inhibiting Rac and/or Rho (50–54).

Advantages of Photoactivation of Phosphopeptides in Cell Biology—Chemical probes, including peptides and proteins that can be activated at will, are powerful tools to study signal transduction in dynamic processes like cell migration. Caged phosphotyrosine peptides are examples of such probes, as they can be introduced into cells in an inactive form and subsequently activated by UV light, producing a temporally and, in some cases, spatially controlled biological response. Utilization of caged phosphopeptides provides several technical advantages in *in situ* studies of signal transduction. The caged group attached directly to the phosphotyrosine increases the stability of the peptide by protecting it from endogenous protein tyrosine phosphatases. Additionally, the phosphopeptide remains in an "inactive" state until the photoactivation step, allowing precise timing of the perturbation. Because the caged phosphopeptides are inactive, each cell can serve as its own control for microinjection.

Nevertheless, challenges remain. It is clear from these studies that the use of short caged phosphopeptides as cellular probes may introduce ambiguity into the studies, because the limited binding determinants of the peptides may not faithfully reflect the behavior of the intact proteins upon which they are patterned. Thus, recent emphasis has been placed on the development of a general methodology for the incorporation of caged phosphoamino acids into native proteins via the suppressor tRNA methodology (55); in the future, this should expand the scope of the caged phosphoprotein-based strategies for probing signal transduction events in cell migration. An additional interpretational limitation is the determination of the absolute amount of peptide microinjected. This measurement is also important for quantitative modeling studies. However, the absolute amount of peptide loaded is difficult to measure directly because there are no convenient assays apart from the actual bioassay consisting of a changed migratory phenotype. In the future, we will concentrate on characterizing peptides conjugated to a fluorophore or caged fluorophore. The fluorescent signal from such peptides could be used directly in single cell concentration assays or in single cell fluorescence correlation spectroscopy measurements to determine concentration. Such efforts are extremely important, but they will involve characterization of essentially new peptides with different solubility, binding, and photochemical properties. Our studies show that defined intervention by the photoactivation methodology in signal transduction networks is an attractive method to test various hypotheses. However, to make the mechanistic connection between a given phenotype and the signaling network involved, more knowledge of relative functional significance of pathways downstream of the uncaging intervention will be required.

REFERENCES

1. Sastry, S. K., and Burridge, K. (2000) *Exp. Cell Res.* **261,** 25–36
2. Zamir, E., and Geiger, B. (2001) *J. Cell Sci.* **114,** 3583–3590
3. Ilic, D., Furuta, Y., Kanazawa, S., Takeda, N., Sobue, K., Nakatsuji, N., Nomura, S., Fujimoto, J., Okada, M., Yamamoto, T., and Aizawa, S. (1995) *Nature* **377,** 539–544
4. Owen, J. D., Ruest, P. J., Fry, D. W., and Hanks, S. K. (1999) *Mol. Cell. Biol.* **19,** 4806–4818
5. Sieg, D. J., Hauck, C. R., and Schlaepfer, D. D. (1999) *J. Cell Sci.* **112,** 2677–2691
6. Cary, L. A., Chang, J. F., and Guan, J. L. (1996) *J. Cell Sci.* **109,** 1787–1794
7. Schaller, M. D., Hildebrand, J. D., Shannon, J. D., Fox, J. W., Vines, R. R., and Parsons, J. T. (1994) *Mol. Cell. Biol.* **14,** 1680–1688
8. Xing, Z., Chen, H. C., Nowlen, J. K., Taylor, S. J., Shalloway, D., and Guan, J. L. (1994) *Mol. Biol. Cell* **5,** 413–421
9. Wells, A., Ware, M. F., Allen, F. D., and Lauffenburger, D. A. (1999) *Cell Motil. Cytoskeleton* **44,** 227–233
10. Zhang, X., Chattopadhyay, A., Ji, Q. S., Owen, J. D., Ruest, P. J., Carpenter, G., and Hanks, S. K. (1999) *Proc. Natl. Acad. Sci. U. S. A.* **96,** 9021–9026
11. Chen, H. C., Appeddu, P. A., Isoda, H., and Guan, J. L. (1996) *J. Biol. Chem.* **271,** 26329–26334
12. Han, D. C., and Guan, J. L. (1999) *J. Biol. Chem.* **274,** 24425–24430
13. Han, D. C., Shen, T. L., and Guan, J. L. (2000) *J. Biol. Chem.* **275,** 28911–28917
14. Shen, T. L., Han, D. C., and Guan, J. L. (2002) *J. Biol. Chem.* **277,** 29069–29077
15. Goicoechea, S. M., Tu, Y., Hua, Y., Chen, K., Shen, T. L., Guan, J. L., and Wu, C. (2002) *Int. J. Biochem. Cell Biol.* **34,** 791–805
16. Schlaepfer, D. D., Jones, K. C., and Hunter, T. (1998) *Mol. Cell. Biol.* **18,** 2571–2585
17. Thomas, J. W., Ellis, B., Boerner, R. J., Knight, W. B., White, G. C., and Schaller, M. D. (1998) *J. Biol. Chem.* **273,** 577–583
18. Humphrey, D., Rajfur, Z., Imperiali, B., Marriott, G., Roy, P., and Jacobson, K. (2005) in *Live Cell Imaging: A Laboratory Manual* (Spector, D. L., and Goldman, R. D., eds) pp. 159–176, Cold Spring Harbor Laboratory Press, Cold Spring Harbor, NY
19. Kaplan, J. H., Forbush, B., III, and Hoffman, J. F. (1978) *Biochemistry* **17,** 1929–1935
20. Park, C.-H., and Givens, R. S. (1997) *J. Am. Chem. Soc.* **119,** 2453–2463
21. Walker, J. W., Gilbert, S. H., Drummond, R. M., Yamada, M., Sreekumar, R., Carraway, R. E., Ikebe, M., and Fay, F. S. (1998) *Proc. Natl. Acad. Sci. U. S. A.* **95,** 1568–1573
22. Roy, P., Rajfur, Z., Jones, D., Marriott, G., Loew, L., and Jacobson, K. (2001) *J. Cell Biol.* **153,** 1035–1048
23. Ghosh, M., Ichetovkin, I., Song, X., Condeelis, J. S., and Lawrence, D. S. (2002) *J. Am. Chem. Soc.* **124,** 2440–2441
24. Ghosh, M., Song, X., Mouneimne, G., Sidani, M., Lawrence, D. S., and Condeelis, J. S. (2004) *Science* **304,** 743–746
25. Rothman, D. M., Vazquez, M. E., Vogel, E. M., and Imperiali, B. (2003) *J. Org. Chem.* **68,** 6795–6798
26. Hancock, W. S., and Battersby, J. E. (1976) *Anal. Biochem.* **71,** 260–264
27. Smith, D. B., and Johnson, K. (1988) *Gene* **67,** 31–40
28. Reynolds, A. B., Roesel, D. J., Kanner, S. B., and Parsons, J. T. (1989) *Mol. Cell Biol.* **9,** 629–638
29. Schaller, M. D., Borgman, C. A., and Parsons, J. T. (1993) *Mol. Cell Biol.* **13,** 785–791
30. Thomas, J. W., Cooley, M. A., Broome, J. M., Salgia, R., Griffin, J. D., Lombardo, C. R., and Schaller, M. D. (1999) *J. Biol. Chem.* **274,** 36684–36692
31. Laemmli, U. K. (1970) *Nature* **227,** 680–685
32. Yeh, R. H., Yan, X., Cammer, M., Bresnick, A. R., and Lawrence, D. S. (2002) *J. Biol. Chem.* **277,** 11527–11532
33. Rothman, D. M., Vazquez, M. E., Vogel, E. M., and Imperiali, B. (2002) *Org. Lett.* **4,** 2865–2868
34. Gilmer, T., Rodriquez, M., Jordan, S., Crosby, R., Alligood, K., Green, M., Kimery, M., Wagner, C., Kinder, D., Charifson, P., Hassell, A. M., Willard, D., Luther, M., Rusnak, D., Sternbach, D. D., Mehrotra, M., Peel, M., Shampine, L., Davis, R., Robbins, J., Patel, I. R., Kassel, D., Burkhart, W., Moyer, M., Bradshaw, T., and Berman, J. (1994) *J. Biol. Chem.* **269,** 31711–31719
35. Reiske, H. R., Kao, S. C., Cary, L. A., Guan, J. L., Lai, J. F., and Chen, H. C. (1999) *J. Biol. Chem.* **274,** 12361–12366
36. Songyang, Z., Shoelson, S. E., Chaudhuri, M., Gish, G., Pawson, T., Haser, W. G., King, F., Roberts, T., Ratnofsky, S., Lechleider, R. J., Neel, B. G., Birge, R. B., Fajardo, J. E., Chou, M. M., Hidesaburo, H., Schaffhausen, B., and Cantley, L. C. (1993) *Cell* **72,** 767–778
37. Waksman, G., Shoelson, S. E., Pant, N., Cowburn, D., and Kuriyan, J. (1993) *Cell* **72,** 779–790
38. Songyang, Z., Margolis, B., Chaudhuri, M., Shoelson, S. E., and Cantley, L. C. (1995) *J. Biol. Chem.* **270,** 14863–14866
39. Liu, X., Brodeur, S. R., Gish, G., Songyang, Z., Cantley, L. C., Laudano, A. P., and Pawson, T. (1993) *Oncogene* **8,** 1119–1126
40. Alonso, G., Koegl, M., Mazurenko, N., and Courtneidge, S. A. (1995) *J. Biol. Chem.* **270,** 9840–9848
41. Boerner, R. J., Kassel, D. B., Barker, S. C., Ellis, B., DeLacy, P., and Knight, W. B. (1996) *Biochemistry* **35,** 9519–9525
42. Moarefi, I., LaFevre-Bernt, M., Sicheri, F., Huse, M., Lee, C. H., Kuriyan, J., and Miller, W. T. (1997) *Nature* **385,** 650–653
43. Corrie, J. E. T., and Trentham, D. R. (1993) *Biological Applications of Photochemical Switches* (Morrison, H., ed) pp. 243–305, John Wiley and Sons, New York
44. Ladbury, J. E., Lemmon, M. A., Zhou, M., Green, J., Botfield, M. C., and Schlessinger, J. (1995) *Proc. Natl. Acad. Sci. U. S. A.* **92,** 3199–3203
45. de Beus, E., and Jacobson, K. (1998) *Cell Motil. Cytoskeleton* **41,** 126–137
46. Klinghoffer, R. A., Sachsenmaier, C., Cooper, J. A., and Soriano, P. (1999) *EMBO J.* **18,** 2459–2471
47. Cary, L. A., Klinghoffer, R. A., Sachsenmaier, C., and Cooper, J. A. (2002) *Mol. Cell. Biol.* **22,** 2427–2440

48. Cantrell, D. A. (2001) *J. Cell Sci.* **114,** 1439–1445
49. Cantley, L. C. (2002) *Science* **296,** 1655–1657
50. Ridley, A. J. (2001) *J. Cell Sci.* **114,** 2713–2722
51. Petit, V., Boyer, B., Lentz, D., Turner, C. E., Thiery, J. P., and Valles, A. M. (2000) *J. Cell Biol.* **148,** 957–970
52. Ren, X. D., Kiosses, W. B., Sieg, D. J., Otey, C. A., Schlaepfer, D. D., and Schwartz, M. A. (2000) *J. Cell Sci.* **113,** 3673–3678
53. Arthur, W. T., Petch, L. A., and Burridge, K. (2000) *Curr. Biol.* **10,** 719–722
54. Chen, B. H., Tzen, J. T., Bresnick, A. R., and Chen, H. C. (2002) *J. Biol. Chem.* **277,** 33857–33863
55. Rothman, D. M., Petersson, E. J., Vazquez, M. E., Brandt, G. S., Dougherty, D. A., and Imperiali, B. (2005) *J. Am. Chem. Soc.* **127,** 846–847